Monthly Notices
of the
ROYAL ASTRONOMICAL SOCIETY

MNRAS **500,** 2227–2235 (2021)
Advance Access publication 2020 November 7

doi:10.1093/mnras/staa3426

Kinematic constraints on spatial curvature from supernovae Ia and cosmic chronometers

J. F. Jesus,[1,2]★ R. Valentim,[3]★ P. H. R. S. Moraes[4] and M. Malheiro[5]

[1]*Universidade Estadual Paulista (UNESP), Campus Experimental de Itapeva, Curso de Engenharia Industrial Madeireira - R. Geraldo Alckmin 519, 18409-010 Itapeva, SP, Brazil*
[2]*Universidade Estadual Paulista (UNESP), Faculdade de Engenharia, Guaratinguetá, Departamento de Física e Química - Av. Dr. Ariberto Pereira da Cunha 333, 12516-410 Guaratinguetá, SP, Brazil*
[3]*Departamento de Física, Instituto de Ciências Ambientais, Químicas e Farmacêuticas (ICAQF), Universidade Federal de São Paulo - UNIFESP, Rua São Nicolau no.210, Centro, 09913-030 Diadema - SP, Brazil*
[4]*Instituto de Astronomia, Geofísica e Ciências Atmosféricas, Universidade de São Paulo, Rua do Matão 1226, 05508-090 São Paulo, SP, Brazil*
[5]*Departamento de Física, Instituto Tecnológico de Aeronáutica (ITA), 12228-900 São José dos Campos - SP, Brazil*

Accepted 2020 October 30. Received 2020 October 29; in original form 2020 September 9

ABSTRACT

An approach to estimate the spatial curvature Ω_k from data independently of dynamical models is suggested, through kinematic parametrizations of the comoving distance $[D_C(z)]$ with third-degree polynomial, of the Hubble parameter $[H(z)]$ with a second-degree polynomial and of the deceleration parameter $[q(z)]$ with first-order polynomial. All these parametrizations were done as function of redshift z. We used SNe Ia data set from Pantheon compilation with 1048 distance moduli estimated in the range $0.01 < z < 2.3$ with systematic and statistical errors and a compilation of 31 $H(z)$ data estimated from cosmic chronometers. The spatial curvature found for $D_C(z)$ parametrization was $\Omega_k = -0.03^{+0.24+0.56}_{-0.30-0.53}$. The parametrization for deceleration parameter $q(z)$ resulted in $\Omega_k = -0.08^{+0.21+0.54}_{-0.27-0.45}$. The $H(z)$ parametrization has shown incompatibilities between $H(z)$ and SNe Ia data constraints, so these analyses were not combined. The $D_C(z)$ and $q(z)$ parametrizations are compatible with the spatially flat universe as predicted by many inflation models and data from cosmic microwave background. This type of analysis is very appealing as it avoids any bias because it does not depend on assumptions about the matter content of the Universe for estimating Ω_k.

Key words: methods: statistical – cosmological parameters – cosmology: observations.

1 INTRODUCTION

The evidence that the Universe is accelerated first came from Supernovae Ia (SNe Ia) observations (Riess et al. 1998; Perlmutter et al. 1999; Astier et al. 2006; Davis et al. 2007; Riess et al. 2007; Kowalski et al. 2008; Amanullah et al. 2010; Suzuki et al. 2012) and was subsequently complemented by data from cosmic microwave background (CMB) radiation (Komatsu et al. 2011; Larson et al. 2011; Planck Collaboration XVI 2014), baryonic acoustic oscillations (BAO; Eisenstein et al. 2005; Percival et al. 2007; Schlegel, White & Eisenstein 2009; Eisenstein et al. 2011; Dawson et al. 2013), and the Hubble parameter $H(z)$ data (Farooq & Ratra 2013; Farooq, Mania & Ratra 2013; Farooq et al. 2017). The acceleration phase of the Universe can be supported by a simple theoretical model using the cosmological constant Λ plus cold dark matter component (Davis et al. 1985; Bertone & Silk 2010; Weinberg et al. 2013). This model has cosmological parameters that have been restricted more and more, and have become very precise by observational data (Planck Collaboration XVI 2014; Farooq & Ratra 2013; Sharov & Vorontsova 2014).

In addition to the 'standard' model that emerges from Λ in the context of cold dark matter, other models have been proposed to explain the problem of accelerated expansion of the Universe. Many of these models have as their main idea, a dark energy fluid that produces a negative pressure that would fill the Universe (Peebles & Ratra 2003; Sahni & Starobinsky 2006). Many hypotheses suggest the nature of this unknown fluid as scalar fields and quintessential models (Amendola 2000; Chiba, Okabe & Yamaguchi 2000; Sahni & Wang 2000; Capozziello & Fang 2002; Khurshudyan, Chubaryan & Pourhassan 2014). Other approaches dealing with accelerated expansion come from modified gravity theories (Volkov 2012), $f(R)$ and $f(T)$, with R and T being the Ricci and energy–momentum trace scalars (Harko et al. 2011; Moraes 2019), respectively, which generalize the general theory of relativity (Sotiriou & Faraoni 2010; Capozziello & de Laurentis 2011; Guo & Frolov 2013), are also investigated; models based on extra dimensions: as models of the braneworld (Cline, Grojean & Servant 1999; Randall & Sundrum 1999; Binetruy & Langlois 2000; Falkowski, Lalak & Pokorski 2000; Shiromizu, Maeda & Sasaki 2000), strings (Damour & Polyakov 1994) and Kaluza–Klein (Overduin & Wesson 1997), among other works. Having adopted a specific model, cosmological parameters can be determined based on statistical analysis of observational data. All of these suggested hypotheses need first of all to be shifted through observational data. This is the way to study cosmology in the present times.

On the other hand, some works attempt to investigate the history of the Universe independently of dynamical models. These

★ E-mail: jf.jesus@unesp.br (JFJ); valentim.rodolfo@unifesp.br (RV)

approaches are called cosmography models or cosmokinetic models (Visser 2004, 2005; Blandford et al. 2005; Elgarøy & Multamäki 2006a; Shapiro & Turner 2006; Rapetti et al. 2007). The work of Capozziello, D'Agostino & Luongo (2020) suggests comparing two different parametrizations: auxiliary variables versus Padé polynomials for high redshifts. Both approaches are made in the context of cosmography, where the scale parameter a is expanded on Taylor series at the present time t_0. This work compares both analysis through the Akaike information criterion and the BIC and showed that the parametrization from the Padé expansion was more promising in the estimate of H_0, q and j.

In this paper, we will refer to them only as kinematic models, whose name comes from the idea that the Universe expansion (or its kinematics) is described by the Hubble expansion rate $H = \frac{\dot{a}}{a}$, deceleration parameter $q = -\ddot{a}a/\dot{a}^2$ and the jerk parameter $j = -\dddot{a}a^3/(a\dot{a}^3)$, where a is the Friedmann–Lemaître–Robertson–Walker (FLRW) metric scale factor. That is, this approach relies only on the cosmological principle, which states that the Universe is statistically homogeneous and isotropic at large scales. Assuming an FLRW metric, which is exactly homogeneous and isotropic, one then looks for hints of $a(t)$ evolution directly from data. In this parametrization, dark matter dominated the $q = 1/2$ universe, while the ΛCDM accelerated model has $j = -1$. These analyses allow us to study the transition from decelerated to accelerated phases, while the j parameter allows you to study deviations from the cosmic concordance model without the restriction of a specific model.

There are several works in the literature that estimated cosmological parameters independently of energy content, in which some authors used parametrization in these estimates (Mortsell & Jonsson 2011; Yu & Wang 2016). In (Sapone, Majerotto & Nesseris 2014), an expansion of the comoving distance was made, as a function of Ω_k, while (L'Huillier & Shafieloo 2017) reconstructed the luminosity distance with a lognormal kernel using data from BAO and SNeIa (BOSS DROSS 12 and JLA). Furthermore, in (Wei & Wu 2017) the distance modulus $\mu_H(z)$ was reconstructed from $H(z)$ data using Gaussian processes (GP) and compared with $\mu_{\rm SN}(z)$ from SNe Ia to estimate Ω_k. In Heavens, Jimenez & Verde (2014), Ω_k is estimated from BAO data regardless of the model. Other parameters were used by (Montanari & Räsänen 2017) to analyse the consistency conditions of FRW. And other authors, such as Collett, Montanari & Räsänen (2019) and Liao et al. (2019) estimated the values of H_0 and Ω_k from gravity lensing data and SNe Ia data where the latter used GP.

All these parametrizations help to reconstruct the Universe evolution without mentioning the dynamics, that is, without the use of Einstein's Equations. Furthermore, using the FLRW metric geometry, we may relate these parametrizations ($H(z)$, $q(z)$) to spatial curvature and cosmological distances: luminosity distance ($d_{\rm L}$) and angular diameter distance (d_A). So, using distance data, like the ones provided by SNe Ia, one may constrain spatial curvature, without assuming any particular Cosmology dynamics. This was first shown by Clarkson, Bassett & Lu (2008).

A first test of this method was done by Mörtsell and Clarkson (Mörtsell & Clarkson 2009). Using only SNe Ia data and three parametrizations of $q(z)$, namely, constant, piecewise and linear on a, they have shown that the Universe is currently accelerating regardless of spatial curvature, but could not conclude about an early expansion deceleration. By combining SNe Ia data with BAO, they concluded that the Universe could have early deceleration only for a flat or open universe ($\Omega_k \geq 0$). It has been shown that future 21 cm intensity experiments can improve model-independent determinations of the spatial curvature (Witzemann et al. 2018).

Yu, Ratra & Wang (2018) have compiled 36 data of $H(z)$, where 31 are measured using the chronometric technique, while five come from BAO (Baryon Acoustic Oscillations) observations. This work used GP to estimate the continuous function of $H(z)$ with values of H_0, z_t, and Ω_k to test the ΛCDM model. They have found $H_0 = 67 \pm 4\,{\rm km\,s^{-1}Mpc^{-1}}$. Using the profile of $H(z)$ function, they estimate limits for the curvature parameter Ω_k. It was found that the transition from deceleration to acceleration redshift is $0.33 < z_t < 1.0$ to 1σ of significance and the value of $\Omega_k = -0.03 \pm 0.11$, which is consistent with a spatially flat universe. The work of Handley (2019) suggests moderate preference for closed universes against flat universe. Di Valentino, Melchiorri & Silk (2020) argue that there is a crisis in cosmology due to interval values of Ω_k obtained from Planck Legacy 2018 (PL2018), $-0.095 < \Omega_k < -0.007$, incompatible with a spatially flat universe, at more than 99 per cent C.l.

In this work, we study the spatial curvature by means of a third-order parametrization of the comoving distance, a second-order parametrization of $H(z)$ and a linear parametrization of $q(z)$. By combining luminosity distances from SNe Ia (Scolnic et al. 2018) and $H(z)$ measurements (Magaña et al. 2018), it is possible to determine Ω_k values in these cosmological models, independently of the matter content of the Universe. In this type of approach, we obtain an interesting complementarity between the observational data and, consequently, tighter constraints on the parameter spaces.

The paper is organized as follows. In Section 2, we present the basic equations concerning the obtainment of Ω_k from comoving distance, $H(z)$ and $q(z)$. Section 3 presents the data set used and the analyses are presented in Section 4. Conclusions are left to Section 5.

2 BASIC EQUATIONS

For general cosmologies, the spatial curvature could not be constrained from a simple parametrization of the cosmological observables. However, as curvature relates to geometry, if one parametrizes the dynamics, the geometry can be constrained through the relation among distances and dynamic observables. To realize this, let us assume as a premise the validity of the cosmological principle, which leads us to the FLRW metric:

$$ds^2 = -dt^2 + a(t)^2\left[\frac{dr^2}{1-kr^2} + r^2(d\theta^2 + \sin^2\theta d\phi^2)\right]. \quad (1)$$

In the context of the FLRW metric, the line-of-sight distance can be estimated. This is the distance between two objects in the Universe that remain constant if the objects are moving with the Hubble flow (Hogg 1999). The line-of-sight comoving distance between an object in redshift z and us is given by

$$d_C = d_{\rm H}\int_0^z \frac{dz'}{E(z')}, \quad (2)$$

where $d_{\rm H} \equiv \frac{c}{H_0}$ is the Hubble distance and the dimensionless Hubble parameter $E(z) \equiv \frac{H(z)}{H_0}$. As all cosmological distances scale with $d_{\rm H}$, we shall adopt the notation where a distance written in upper case (D_i) is dimensionless, while a distance written in lower case (d_i) is dimensionful and $d_i \equiv d_{\rm H}D_i$. So, we may write

$$D_{\rm C}(z) = \int_0^z \frac{dz'}{E(z')}. \quad (3)$$

From this, we may obtain the transverse comoving distance. The comoving distance between two events at the same redshift but separated on the sky by some angle $\delta\theta$ is $d_{\rm M}\delta\theta$ and the

transverse comoving distance is related to the line-of-sight comoving distance as

$$d_{\rm M} = d_{\rm H} \begin{cases} \frac{1}{\sqrt{\Omega_k}} \sinh\left[\sqrt{\Omega_k} D_{\rm C}\right] & \text{for } \Omega_k > 0, \\ D_{\rm C} & \text{for } \Omega_k = 0, \\ \frac{1}{\sqrt{-\Omega_k}} \sin\left[\sqrt{-\Omega_k} D_{\rm C}\right] & \text{for } \Omega_k < 0. \end{cases} \tag{4}$$

where we have used the curvature parameter density $\Omega_k \equiv -\frac{k}{a_0^2 H_0^2}$. By defining the following function

$$\mathrm{sinn}\,(x, \Omega_k) \equiv \begin{cases} \frac{1}{\sqrt{\Omega_k}} \sinh\left[x\sqrt{\Omega_k}\right] & \text{for } \Omega_k > 0, \\ x & \text{for } \Omega_k = 0, \\ \frac{1}{\sqrt{-\Omega_k}} \sin\left[x\sqrt{-\Omega_k}\right] & \text{for } \Omega_k < 0, \end{cases} \tag{5}$$

equation (4) can be simplified as

$$d_{\rm M} = d_{\rm H}\,\mathrm{sinn}\,(D_{\rm C}, \Omega_k). \tag{6}$$

The luminosity distance $d_{\rm L}$ is defined by the relationship between bolometric flux S and bolometric luminosity L:

$$d_{\rm L} = \sqrt{\frac{L}{4\pi S}}. \tag{7}$$

We may relate it to the transverse comoving distance by

$$D_{\rm L}(z) = (1+z) D_{\rm M}(z). \tag{8}$$

We shall briefly mention the dynamics here just to show how the curvature density parameter definition emerges. As it is well known, the Friedmann equations can be written as

$$H^2 = \frac{8\pi G \rho_{\rm T}}{3} - \frac{k}{a^2}, \tag{9}$$

$$\frac{\ddot{a}}{a} = \dot{H} + H^2 = -\frac{4\pi G}{3}(\rho_{\rm T} + 3p_{\rm T}), \tag{10}$$

where $\rho_{\rm T}$ represents the total energy density and $p_{\rm T}$ the total pressure. As it can be seen, the spatial curvature contributes to the Hubble parameter through equation (9), while it does not contribute to acceleration ($\ddot{a}$) explicitly (10). The Friedmann equation shows that if we know the matter-energy content of the Universe, we can estimate its spatial curvature. This can be clearly seen if we rewrite equation (9) as

$$\Omega_T + \Omega_k = 1\,, \tag{11}$$

where $\Omega_T \equiv \frac{8\pi G \rho_T}{3H^2}$ is the total energy density parameter and $\Omega_k \equiv -\frac{k}{a^2 H^2}$ is the curvature parameter.

Here, we intend to obtain constraints over spatial curvature without making any assumptions about the matter-energy content of the Universe. Thus, we shall assume kinematic expressions for the observables like $H(z)$, $q(z)$, and $D_{\rm C}(z)$.

Assuming this kinematic approach, we can see that $H(z)$ data alone cannot constrain spatial curvature, but luminosity distances from SNe Ia can constrain it through the Ω_k dependence in equation (4). Concerning the deceleration parameter $q(z)$, it can be given as

$$q(z) = -\frac{\ddot{a}}{aH^2} = \frac{1+z}{H}\frac{{\rm d}H}{{\rm d}z} - 1\,, \tag{12}$$

So, as expected from equation (10), a $q(z)$ kinematical parametrization will not depend explicitly on spatial curvature, however, the spatial curvature can be constrained through the distance relation (4).

Therefore, we may access the value of Ω_k through a parametrization of both $q(z)$ and $H(z)$. As a third method, we can also parametrize the line-of-sight comoving distance, which is directly related to the luminosity distance, in order to obtain the spatial curvature. In what follows we present the three different methods considered here.

Table 1. Bayesian information criterion.

ΔBIC	Support
$\Delta\mathrm{BIC} \leq 1$	No worth more than a bare mention
$1 \leq \Delta\mathrm{BIC} \leq 3$	Significant/weak
$3 \leq \Delta\mathrm{BIC} \leq 5$	Strong to very strong/significant
$\Delta\mathrm{BIC} > 5$	Decisive/strong

2.1 Choice of parametric functions for $D_{\rm C}(z)$, $H(z)$, and $q(z)$

We shall perform a model selection in order to find the ideal polynomial that better describes the data for the $D_{\rm C}$, H, and q parametrizations. The best Bayesian tool for model selection is Bayesian Evidence (Kass & Raftery 1995; Elgarøy & Multamäki 2006b; Guimarães, Cunha & Lima 2009; Jesus, Valentim & Andrade-Oliveira 2017). However, the Bayesian Evidence, in general, is given by multidimensional integrals over the parameters, so it is usually hard to evaluate. A way around this difficulty is using its approximation, first obtained by Schwarz (Schwarz 1978; Liddle 2004), known as BIC. BIC (Valentim, Rangel & Horvath 2011b; Valentim, Horvath & Rangel 2011a; Szydłowski et al. 2015) heavily penalizes models with different number of free parameters.

Here, we use BIC in order to find the ideal polynomial order in each of the parametrizations aiming to find model-independent constraints on spatial curvature. The BIC is given by

$$\mathrm{BIC} = -2\ln\mathcal{L}_{\rm max} + p\ln N\,, \tag{13}$$

where p is the number of free parameters and N is the number of data. As the likelihood is given by

$$\mathcal{L} = e^{-\frac{\chi^2}{2}}\,, \tag{14}$$

then, we may write

$$\mathrm{BIC} = \chi^2_{\rm min} + p\ln N\,. \tag{15}$$

The interpretation of ΔBIC outcomes is described in Table 1.

The results for the three parametrizations can be seen on Table 2.

As can be seen on Table 2, the ideal polynomial order for $D_{\rm C}(z)$, $H(z)$, and $q(z)$ are 2, 2 and 1, respectively. However, for $D_{\rm C}(z)$, the third-degree polynomial can not be discarded by this analysis ($\Delta\mathrm{BIC} < 1$). We have tested the second-degree parametrization for $D_{\rm C}(z)$ and have found a too close universe ($\Omega_k = -0.49 \pm 0.14$ at 68 per cent C.l.), which was in disagreement with the $q(z)$ parametrizations and with other data, like CMB (Planck Collaboration VI 2018). As the third-order parametrization can not be discarded by this analysis, we chose to work with this order for $D_{\rm C}(z)$.

2.2 Ω_k from line-of-sight comoving distance, $D_{\rm C}(z)$

In order to put limits on Ω_k by considering the line-of-sight comoving distance, we can write $D_{\rm C}(z)$ as a third-degree polynomial such as

$$D_{\rm C} = z + d_2 z^2 + d_3 z^3, \tag{16}$$

where d_2 and d_3 are free parameters. From equation (2), we may write

$$E(z) = \left[\frac{{\rm d}D_{\rm C}(z)}{{\rm d}z}\right]^{-1}. \tag{17}$$

Naturally, from equations (16) and (17), one obtains

$$E(z) = \frac{1}{1 + 2d_2 z + 3d_3 z^2}\,. \tag{18}$$

Table 2. Bayesian model comparison for different parametrizations.

Parametrization	Polynomial order	χ^2_{min}	χ^2_{red}	BIC	ΔBIC
$D_C(z)$	1	1250.825	1.16140	1264.793	+ 193.915
	2	1049.927	0.97577	1070.878	0
	3	1043.839	0.97101	1071.775	+ 0.897
	4	1042.471	0.97064	1077.390	+ 6.512
$H(z)$	1	1059.386	0.98456	1080.338	+ 9.253
	2	1043.150	0.97037	1071.085	0
	3	1042.975	0.97111	1077.894	+ 6.809
$q(z)$	0	1066.636	0.99130	1087.588	+ 16.036
	1	1043.617	0.97081	1071.552	0
	2	1042.919	0.97106	1077.838	+ 6.286
	3	1042.375	0.97146	1084.278	+ 12.726

Finally, from equations (8), (16), and (6) the dimensionless luminosity distance is

$$D_L(z) = (1+z)\,\mathrm{sinn}\left(z + d_2 z^2 + d_3 z^3, \Omega_k\right). \tag{19}$$

Equations (18) and (19) shall be compared with $H(z)$ measurements and luminosity distances from SNe Ia, respectively, in order to determine d_2 and Ω_k.

2.3 Ω_k from $H(z)$

In order to assess Ω_k by means of $H(z)$, we need an expression for $H(z)$. If one wants to avoid dynamical assumptions, one must resort to kinematical methods which use an expansion of $H(z)$ over the redshift.

Let us try a simple $H(z)$ expansion, namely, the quadratic expansion:

$$\frac{H(z)}{H_0} = E(z) = 1 + h_1 z + h_2 z^2. \tag{20}$$

In order to constrain the model with SNe Ia data, we obtain the luminosity distance from equations (3), (8), and (20). We have

$$D_C = \int_0^z \frac{\mathrm{d}z'}{E(z')} = \int_0^z \frac{\mathrm{d}z'}{1 + h_1 z' + h_2 z'^2}, \tag{21}$$

which gives three possible solutions, according to the sign of $\Delta \equiv h_1^2 - 4h_2$, such as

$$D_C = \begin{cases} \frac{2}{\sqrt{-\Delta}}\left[\arctan\left(\frac{2h_2 z + h_1}{\sqrt{-\Delta}}\right) - \arctan\frac{h_1}{\sqrt{-\Delta}}\right], & \Delta < 0, \\ \frac{2z}{h_1 z + 2}, & \Delta = 0, \\ \frac{1}{\sqrt{\Delta}} \ln\left|\left(\frac{\sqrt{\Delta}+h_1}{\sqrt{\Delta}-h_1}\right)\left(\frac{\sqrt{\Delta}-h_1-2h_2 z}{\sqrt{\Delta}+h_1+2h_2 z}\right)\right|, & \Delta > 0, \end{cases} \tag{22}$$

from which follows the luminosity distance $D_L(z) = (1+z)\,\mathrm{sinn}\,(D_C, \Omega_k)$.

2.4 Ω_k from $q(z)$

Now, we can analyse Ω_k by parametrizing $q(z)$. From (12) one may find $E(z)$ as

$$E(z) = \exp\left[\int_0^z \frac{1+q(z')}{1+z'}\mathrm{d}z'\right]. \tag{23}$$

If we assume a linear z dependence in $q(z)$, as

$$q(z) = q_0 + q_1 z, \tag{24}$$

which is the simplest $q(z)$ parametrization that allows for an acceleration transition as required by SNe Ia data (Riess et al. 2004; Lima et al. 2012), one may find

$$E(z) = e^{q_1 z}(1+z)^{1+q_0-q_1}, \tag{25}$$

while the line-of-sight comoving distance $D_C(z)$ (3) is given by

$$D_C(z) = e^{q_1} q_1^{q_0-q_1}\left[\Gamma(q_1 - q_0, q_1) - \Gamma(q_1 - q_0, q_1(1+z))\right], \tag{26}$$

where $\Gamma(a, x)$ is the incomplete gamma function defined in Abramowitz, Stegun & Romer (1988) as $\Gamma(a,x) \equiv \int_x^\infty e^{-t} t^{a-1}\mathrm{d}t$, with $a > 0$, from which follows the luminosity distance as $D_L(z) = (1+z)\,\mathrm{sinn}\,(D_C, \Omega_k)$, which can be constrained from observational data.

3 SAMPLES

3.1 $H(z)$ data set

In order to constrain the free parameters, we use the Hubble parameter ($H(z)$) data in different redshift values. These kind of observational data are quite reliable because in general such observational data are independent of the background cosmological model, just relying on astrophysical assumptions. We have used the currently most complete compilation of $H(z)$ data, with 51 measurements (Magaña et al. 2018).

At the present time, the most important methods for obtaining $H(z)$ data are[1] (i) through 'cosmic chronometers', for example, the differential age of galaxies (Simon, Verde & Jimenez 2005; Stern et al. 2010; Moresco et al. 2012; Zhang et al. 2014; Moresco 2015; Moresco et al. 2016), (ii) measurements of peaks of acoustic oscillations of baryons (BAO; Gaztañaga, Cabré & Hui 2009; Blake et al. 2012; Busca et al. 2013; Anderson et al. 2014; Font-Ribera et al. 2014; Delubac et al. 2015), and (iii) through correlation function of luminous red galaxies (LRG; Chuang & Wang 2013; Oka et al. 2014).

Among these methods for estimating $H(z)$, the 51 data compilation as grouped by Magaña et al. (2018), consists of 20 clustering (BAO + LRG), and 31 differential age $H(z)$ data.

Differently from Magaña et al. (2018), we choose not to use H_0 in our main results here, due to the current tension among H_0 values estimated from different observations (Riess et al. 2016; Planck Collaboration XIII 2016; Bernal, Verde & Riess 2016).

The method used to estimate $H(z)$ data from BAO depends on the choice of a fiducial cosmological model. Even if it has an weak model dependence, we choose here not to work with the $H(z)$ data from BAO. So, in order to keep the analysis the most model-independent

[1] See (Lima et al. 2012) for a review.

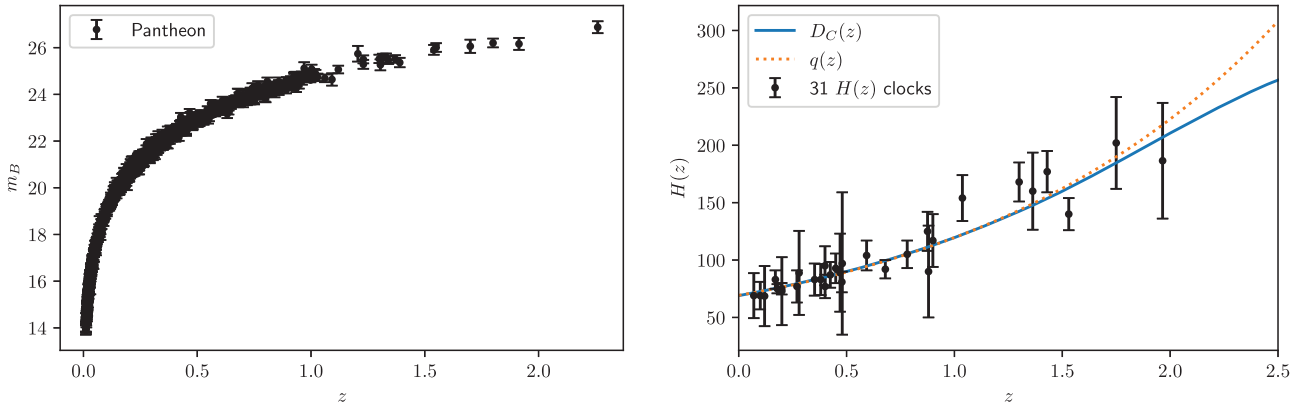

Figure 1. (a) SNe Ia apparent magnitude m_B from Pantheon. The error bars shown correspond only to statistical errors, but we use the full covariance matrix (statistical + systematic errors) in the analysis. (b) 31 $H(z)$ cosmic chronometers. The lines represent the best fit from SNe + $H(z)$ data for each model.

possible, we shall work here only with the 31 differential age $H(z)$ data (cosmic chronometers) from Magaña et al. (2018).

3.2 SNe Ia

We have chosen to work with one of the largest SNe Ia sample to date, namely, the Pantheon sample (Scolnic et al. 2018). This sample consists of 279 SNe Ia from Pan-STARRS1 (PS1) Medium Deep Survey ($0.03 < z < 0.68$), combined with distance estimates of SNe Ia from Sloan Digital Sky Survey, SuperNova Legacy Survey (SNLS) and various low- z and *Hubble Space Telescope* samples to form the largest combined sample of SNe Ia, consisting of a total of 1048 SNe Ia in the range of $0.01 < z < 2.3$.

As explained on Scolnic et al. (2018), the PS1 light-curve fitting has been made with SALT2 (Guy et al. 2010), as it has been trained on the JLA sample (Betoule et al. 2014). Three quantities are determined in the light-curve fit that are needed to derive a distance: the colour c, the light-curve shape parameter x_1, and the log of the overall flux normalization m_B. We can see the m_B data for Pantheon at Fig. 1(a).

The SALT2 light-curve fit parameters are transformed into distances using a modified version of the Tripp formula (Tripp & Branch 1999):

$$\mu = m_B - M + \alpha x_1 - \beta c + \Delta_M + \Delta_B, \tag{27}$$

where μ is the distance modulus, Δ_M is a distance correction term based on the host galaxy mass of the SN, and Δ_B is a distance correction factor based on predicted biases from simulations. As can be seen, α is the coefficient of the relation between luminosity and stretch, while β is the coefficient of the relation between luminosity and colour, and M is the absolute B-band magnitude of a fiducial SN Ia with $x_1 = 0$ and $c = 0$.

Differently from previous SNe Ia samples, like JLA (Betoule et al. 2014), Pantheon uses a calibration method named BEAMS with Bias Corrections, which uses cosmological simulations assuming a reference ΛCDM model. The cosmological dependence is expected to be small, so neglecting this dependence, allows one to determine SNe Ia distances without one having to fit SNe parameters jointly with cosmological parameters. Thus, Pantheon provide directly corrected m_B estimates in order for one to constrain cosmological parameters alone.

The systematic uncertainties were propagated through a systematic uncertainty matrix. An uncertainty matrix C was defined such that

$$C = D_{\rm stat} + C_{\rm sys}. \tag{28}$$

The statistical matrix $D_{\rm stat}$ has only a diagonal component that includes photometric errors of the SN distance, the distance uncertainty from the mass step correction, the uncertainty from the distance bias correction, the uncertainty from the peculiar velocity uncertainty and redshift measurement uncertainty in quadrature, the uncertainty from stochastic gravitational lensing, and the intrinsic scatter.

4 ANALYSES AND RESULTS

In our analyses, we have chosen flat priors for all parameters, so always the posterior distributions are proportional to the likelihoods.

For $H(z)$ data, the likelihood distribution function is given by

$$\mathscr{L}_H \propto e^{-\frac{\chi^2_H}{2}},$$

with

$$\chi^2_H = \sum_{i=1}^{31} \frac{\left[H_{{\rm obs},i} - H(z_i, s)\right]^2}{\sigma^2_{H_i,{\rm obs}}}. \tag{29}$$

The χ^2 function for Pantheon is given by

$$\chi^2_{\rm SN} = \Delta m^T \cdot C^{-1} \cdot \Delta m, \tag{30}$$

where **C** is the same from (28), $\Delta m = m_B - m_{\rm mod}$, and

$$m_{\rm mod} = 5\log_{10} D_L(z) + \mathcal{M}, \tag{31}$$

where $\mathcal{M}$ is a nuisance parameter which encompasses H_0 and M. We choose to project over $\mathcal{M}$, which is equivalent to marginalize the likelihood $\mathscr{L}_{\rm SN} \propto e^{-\chi^2_{\rm SN}/2}$ over $\mathcal{M}$, up to a normalization constant. In this case, we find the projected $\chi^2_{\rm proj}$:

$$\chi^2_{\rm proj} = S_{\rm mm} - \frac{S^2_m}{S_A}, \tag{32}$$

where $S_{\rm mm} = \sum_{i,j} \Delta m_i \Delta m_j A_{ij} = \Delta m^T \cdot A \cdot \Delta m$, $S_m = \sum_{i,j} \Delta m_i A_{ij} = \Delta m^T \cdot A \cdot 1$, $S_A = \sum_{i,j} A_{ij} = 1^T \cdot A \cdot 1$ and $A \equiv C^{-1}$.

In order to obtain the constraints over the free parameters, the likelihood $\mathscr{L} \propto e^{-\chi^2/2}$, where $\chi^2 \equiv \chi^2_H + \chi^2_{proj}$, has been sampled through a Monte Carlo Markov Chain (MCMC) analysis. A simple and powerful MCMC method is the so-called Affine Invariant MCMC Ensemble Sampler by Goodman & Weare (2010), which was implemented in `Python` language with the `emcee` software by Foreman-Mackey et al. (2013).

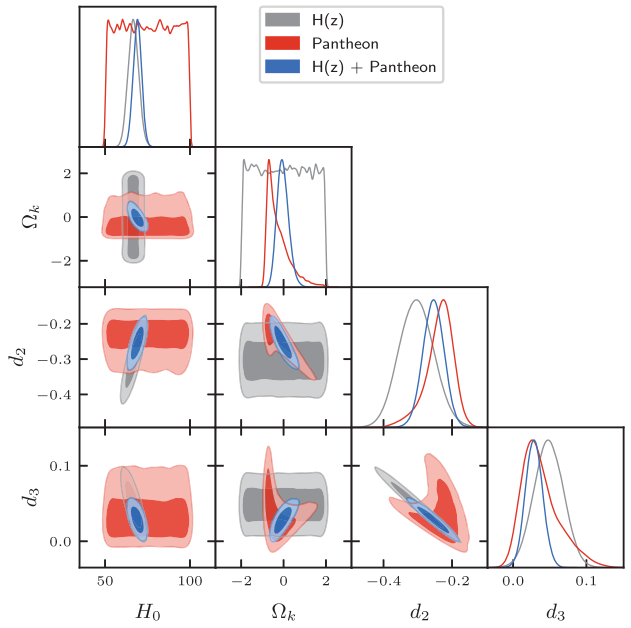

Figure 2. All constraints from Pantheon and cosmic chronometers for $D_C(z) = z + d_2z^2 + d_3z^3$. The contours correspond to 68.3 per cent C.l. and 95.4 per cent C.l.

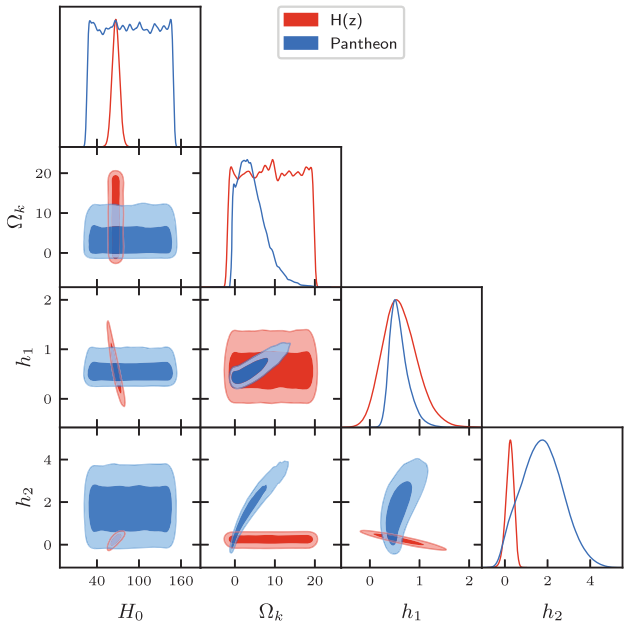

Figure 3. All constraints from Pantheon and cosmic chronometers for $H(z) = H_0(1 + h_1z + h_2z^2)$. The contours correspond to 68.3 per cent C.l. and 95.4 per cent C.l.

We used the free software `emcee` to sample from our likelihood in n-dimensional parameter space. In order to plot all the constraints on each model in the same figure, we have used the freely available software `getdist`,[2] in its `Python` version. The results of our statistical analyses can be seen on Figs 2–7 and on Table 3.

[2]`getdist` is part of the great MCMC sampler and CMB power spectrum solver `COSMOMC`, by (Lewis & Bridle 2002).

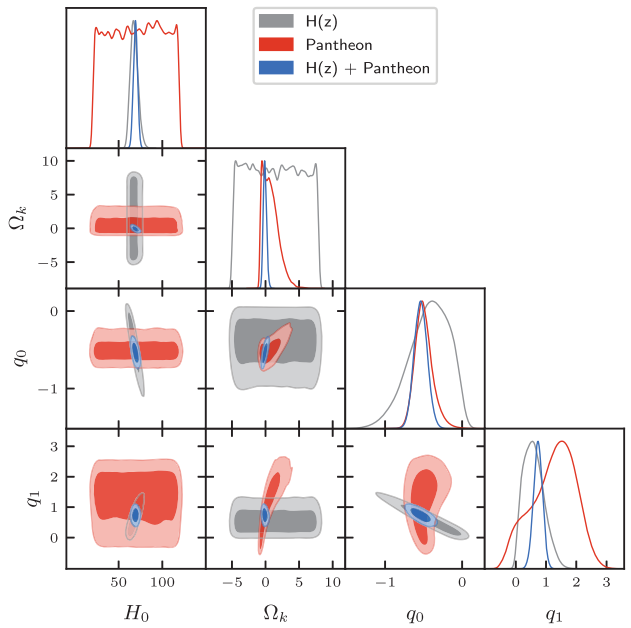

Figure 4. All constraints from Pantheon and cosmic chronometers for $q(z) = q_0 + q_1z$. The contours correspond to 68.3 per cent C.l. and 95.4 per cent C.l.

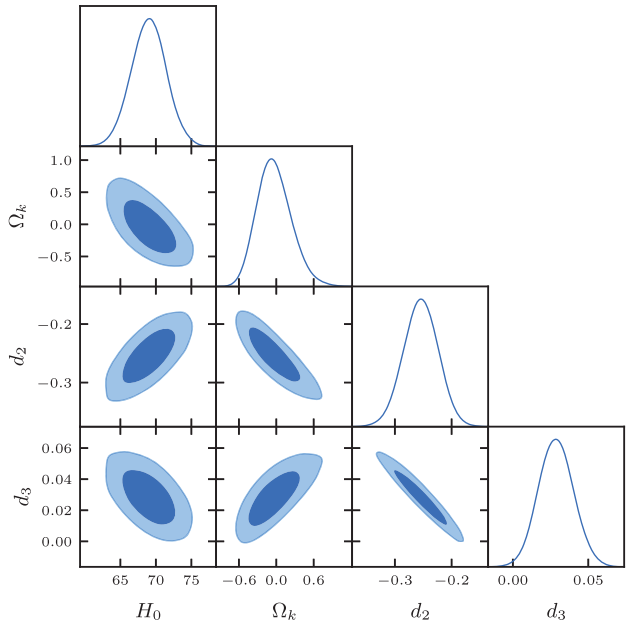

Figure 5. Combined constraints from Pantheon and $H(z)$ for $D_C(z) = z + d_2z^2 + d_3z^3$. The contours correspond to 68.3 per cent C.l. and 95.4 per cent C.l.

In Figs 2–4, we show explicitly the independent constraints, in order to see the complementarity between SNe Ia and $H(z)$ data. First of all, as expected, SNe Ia does not constrain H_0. In SNe confidence level contours, H_0 is only limited by our prior, but $H(z)$ data gives good constraints over H_0. We can see also, that in general, SNe Ia alone does not constrain well Ω_k, but by combining with $H(z)$, which constrain the other parameters, good constraints over the curvature are found. In the planes not containing Ω_k ($d_2 - d_3$, $h_1 - h_2$ and $q_0 - q_1$) we can see that $H(z)$ also helps to reduce a lot the allowed parameter space.

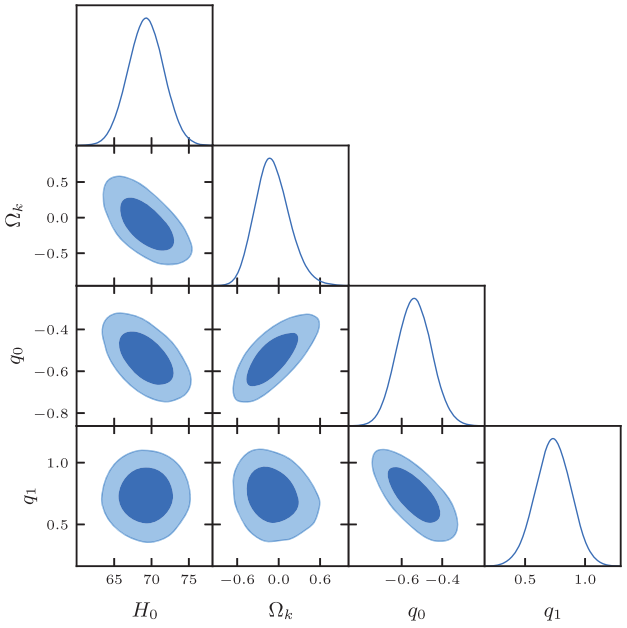

Figure 6. Combined constraints from Pantheon and $H(z)$ for $q(z) = q_0 + q_1 z$. The contours correspond to 68.3 per cent C.l. and 95.4 per cent C.l.

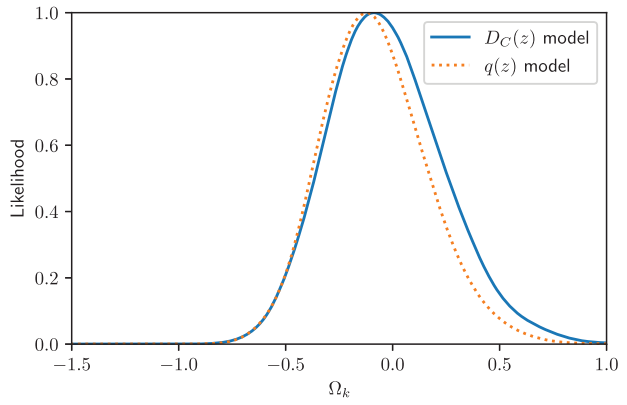

Figure 7. Likelihoods for spatial curvature density parameter from Pantheon and $H(z)$ data combined. The blue solid line corresponds to $D_C(z)$ parametrization, the orange long-dashed line corresponds to $q(z)$ parametrization. $H(z)$ parametrization was not combined, as mentioned in the text.

In Figs 5 and 6, we have the combined results for each parametrization, where we can clearly see how the combination SNe Ia + $H(z)$ yields good constraints over Ω_k, as well as the other kinematic parameters. For all parametrizations, the best constraints over the spatial curvature comes from $q(z)$ model, as can be seen on Fig. 7. We can also see in this figure that all constraints are compatible at 1σ C.l. Finally, Table 3 shows the full numerical results from our statistical analysis.

Comparing with previous results in the literature, Li et al. (2016) have combined 22 $H(z)$ data from cosmic chronometers with Union 2.1 SNe Ia data and JLA SNe Ia data. The combination with Union 2.1 yielded $\Omega_k = -0.045^{+0.176}_{-0.172}$ and they found $\Omega_k = -0.140^{+0.161}_{-0.158}$ from JLA combination. Wang et al. (2017) have put model-independent constraints over Ω_k and opacity from JLA SNe Ia data and 30 $H(z)$ data. They have used GP method and have obtained $\Omega_k = 0.44 \pm 0.64$, with a high uncertainty, due to degeneracy with opacity. It is worth to mention that, although model-independent, both Li et al. (2016) and Wang et al. (2017) have followed a different approach from the present paper. They do not parametrize any cosmological observable, instead they obtain a distance modulus from $H(z)$ data, and compare with distance modulus from SNe Ia, which are dependent on spatial curvature.

Table 3. Constraints from Pantheon + $H(z)$ for $D_C(z)$ and $q(z)$ parametrizations. The central values correspond to the mean and the 1σ and 2σ C.l. correspond to the minimal 68.3% and 95.4% confidence intervals.

Parameter	$D_C(z)$	$q(z)$
H_0	$69.0 \pm 2.4 \pm 4.9$	$69.3 \pm 2.4^{+4.8}_{-4.7}$
Ω_k	$-0.03^{+0.24+0.56}_{-0.30-0.53}$	$-0.08^{+0.21+0.54}_{-0.27-0.45}$
d_2	$-0.255 \pm 0.030^{+0.059}_{-0.061}$	–
d_3	$0.029 \pm 0.011^{+0.023}_{-0.022}$	–
q_0	–	$-0.536 \pm 0.085 \pm 0.17$
q_1	–	$0.73 \pm 0.15 \pm 0.30$

Another interesting reference is Marra & Sapone (2018),[3] where they use a similar formalism, namely, the Linear Model Formalism (Gregory 2005) in order to perform some diagnostics related to the validity of the FLRW geometry and of the the ΛCDM model. One of the diagnostics, the $Ok(z)$ diagnostic (Clarkson et al. 2008), relates directly to Ω_k in the case that the FLRW geometry is valid. They have made a $Ok(z)$ reconstruction compatible with a spatially flat universe, which in turn, is compatible with our present results.

As already mentioned, Yu et al. (2018) have used $H(z)$ and BAO, with the aid of GP and have found $\Omega_k = -0.03 \pm 0.21$, consistent with our results. By combining CMB data with BAO, in the context of ΛCDM, the Planck Collaboration VI (2018) have found $\Omega_k = 0.001 \pm 0.002$. It is consistent with our result, but it is dependent on the chosen dynamical model, ΛCDM.

Another interesting result that can be seen on Table 3 is the H_0 constraint. As one may see, the constraints over H_0 are consistent among both parametrizations. The constraints over H_0 are quite stringent today from many observations (Riess et al. 2019; Planck Collaboration VI 2018). However, there is some tension among H_0 values estimated from Cepheids (Riess et al. 2019) and from CMB (Planck Collaboration VI 2018). While Riess *et al.* advocate $H_0 = 74.03 \pm 1.42\,\mathrm{km\,s^{-1}\,Mpc^{-1}}$, the Planck collaboration analysis, in the context of ΛCDM, yields $H_0 = 67.4 \pm 0.5\,\mathrm{km\,s^{-1}\,Mpc^{-1}}$, a 4.4σ lower value.

It is interesting to note, from our Table 3 that, although we are working with model-independent parametrizations and data at intermediate redshifts, our result is in better agreement with the high-redshift result from Planck. In fact, all our results are compatible within 1σ with the Planck's result, while, for the Riess' result, our $D_C(z)$ result is marginally compatible at 1.8σ, and $q(z)$ is marginally compatible at 1.7σ.

5 CONCLUSIONS

In this work, we wrote the comoving distance D_C, the Hubble parameter $H(z)$, and the deceleration parameter $q(z)$ as the third-, the second-, and the first-degree polynomials on z, respectively (see equations 16, 20, and 24), and obtained, for each case, the Ω_k value. We have shown that by combining Supernovae type Ia data and Hubble parameter measurements, nice constraints are found over

[3] See also von Marttens et al. (2019) for a similar analysis related to a possible interaction in the dark sector.

the spatial curvature, without the need of assuming any particular dynamical model. Our results can be found in Figs 2–6. As one may see from Figs 2–4, the analyses using SNe Ia and $H(z)$ data are complementary to each other, providing tight limits in the parameter spaces. As a result, the values obtained for the spatial curvature in each case were $\Omega_k = -0.03^{+0.24}_{-0.30}$ and $-0.08^{+0.21}_{-0.27}$ at 1σ C.l., for $D_C(z)$ and $q(z)$ parametrizations (see Fig. 7), all compatible with a spatially flat Universe, as predicted by most inflation models and confirmed by CMB data, in the context of ΛCDM model. The $H(z)$ parametrization presented incompatibilities from its constraints coming from SNe Ia and cosmic clocks data and was not considered in the joint analysis.

Further investigations could include different parametrizations and other kinematical methods in order to determine the Universe spatial curvature independently from the matter-energy content.

ACKNOWLEDGEMENTS

JFJ is supported by Fundação de Amparo à Pesquisa do Estado de São Paulo (Fundação de Amparo à Pesquisa do Estado de São Paulo (FAPESP); Process no. 2017/05859-0). RV and MM are supported by FAPESP (thematic project process no. 2013/26258-2 and regular project process no. 2016/09831-0). MM is also supported by Conselho Nacional de Desenvolvimento Científico e Tecnológico (CNPq) and Coordenação de Pessoal de Ensino Superior (CAPES). PHRSM also thanks CAPES for financial support.

DATA AVAILABILITY

No new data were generated or analysed in support of this research.

REFERENCES

Abramowitz M., Stegun I. A., Romer R. H., 1988, Am. J. Phys., 56, 958
Amanullah R. et al., 2010, ApJ, 716, 712
Amendola L., 2000, Phys. Rev. D, 62, 043511
Anderson L. et al., 2014, MNRAS, 439, 83
Astier P. et al., 2006, A&A, 447, 31
Bernal J. L., Verde L., Riess A. G., 2016, J. Cosmol. Astropart. Phys., 2016, 019
Bertone G., Silk J., 2010, Particle Dark Matter. Cambridge Univ. Press, Cambridge, p. 3
Betoule M. et al., 2014, A&A, 568, A22
Binetruy P., Langlois D., 2000, Nucl. Phys. B, 565, 269
Blake C. et al., 2012, MNRAS, 425, 405
Blandford R. D., Amin M., Baltz E. A., Mandel K., Marshall P. J., 2005, in Wolff S. C., Lauer T. R., eds, ASP Conf. Ser. Vol. 339, Observing Dark Energy. Astron. Soc. Pac., San Francisco, p. 27
Busca N. G. et al., 2013, A&A, 552, A96
Capozziello S., de Laurentis M., 2011, Phys. Rep., 509, 167
Capozziello S., Fang L. Z., 2002, Int. J. Mod. Phys. D, 11, 483
Capozziello S., D'Agostino R., Luongo O., 2020, MNRAS, 494, 2576
Chiba T., Okabe T., Yamaguchi M., 2000, Phys. Rev. D, 62, 023511
Chuang C.-H., Wang Y., 2013, MNRAS, 435, 255
Clarkson C., Bassett B., Lu T. H.-C., 2008, Phys. Rev. Lett., 101, 011301
Cline J. M., Grojean C., Servant G., 1999, Phys. Rev. Lett., 83, 4245
Collett T., Montanari F., Räsänen S., 2019, Phys. Rev. Lett., 123, 231101
Damour T., Polyakov A. M., 1994, Gen. Relativ. Gravit., 26, 1171
Davis M., Efstathiou G., Frenk C. S., White S. D. M., 1985, ApJ, 292, 371
Davis T. M. et al., 2007, ApJ, 666, 716
Dawson K. S. et al., 2013, AJ, 145, 10
Delubac T. et al., 2015, A&A, 574, A59
Di Valentino E., Melchiorri A., Silk J., 2020, Nature Astronomy, 4, 196
Eisenstein D. J. et al., 2005, ApJ, 633, 560
Eisenstein D. J. et al., 2011, AJ, 142, 72
Elgarøy Ø., Multamäki T., 2006a, J. Cosmol. Astropart. Phys., 2006, 002
Elgarøy Ø., Multamäki T., 2006b, J. Cosmol. Astropart. Phys., 2006, 002
Falkowski A., Lalak Z., Pokorski S., 2000, Phys. Lett. B, 491, 172
Farooq O., Ratra B., 2013, ApJ, 766, L7
Farooq O., Mania D., Ratra B., 2013, ApJ, 764, 138
Farooq O., Ranjeet Madiyar F., Crandall S., Ratra B., 2017, ApJ, 835, 26
Font-Ribera A. et al., 2014, J. Cosmol. Astropart. Phys., 2014, 027
Foreman-Mackey D., Hogg D. W., Lang D., Goodman J., 2013, PASP, 125, 306
Gaztañaga E., Cabré A., Hui L., 2009, MNRAS, 399, 1663
Goodman J., Weare J., 2010, Commun. Appl. Math. Comput. Sci., 5, 65
Gregory P. C., 2005, Bayesian Logical Data Analysis for the Physical Sciences: A Comparative Approach with 'Mathematica' Support. Cambridge Univ. Press, Cambridge
Guimarães A. C. C., Cunha J. V., Lima J. A. S., 2009, J. Cosmol. Astropart. Phys., 2009, 010
Guo J.-Q., Frolov A. V., 2013, Phys. Rev. D, 88, 124036
Guy J. et al., 2010, A&A, 523, A7
Handley W., 2019, PRL, preprint (arXiv:1908.09139)
Harko T., Lobo F. S. N., Nojiri S., Odintsov S. D., 2011, Phys. Rev. D, 84, 024020
Heavens A., Jimenez R., Verde L., 2014, Phys. Rev. Lett., 113, 241302
Hogg D. W., 1999, preprint (arXiv:astro-ph/9905116)
Jesus J. F., Valentim R., Andrade-Oliveira F., 2017, J. Cosmol. Astropart. Phys., 2017, 030
Kass R. E., Raftery A. E., 1995, J. Am. Stat. Assoc., 90, 773
Khurshudyan M., Chubaryan E., Pourhassan B., 2014, Int. J. Theor. Phys., 53, 2370
Komatsu E. et al., 2011, ApJS, 192, 18
Kowalski M. et al., 2008, ApJ, 686, 749
L'Huillier B., Shafieloo A., 2017, J. Cosmol. Astropart. Phys., 2017, 015
Larson D. et al., 2011, ApJS, 192, 16
Lewis A., Bridle S., 2002, Phys. Rev. D, 66, 103511
Li Z., Wang G.-J., Liao K., Zhu Z.-H., 2016, ApJ, 833, 240
Liao K., Shafieloo A., Keeley R. E., Linder E. V., 2019, ApJ, 886, L23
Liddle A. R., 2004, MNRAS, 351, L49
Lima J. A. S., Jesus J. F., Santos R. C., Gill M. S. S., 2012, preprint (arXiv:1205.4688)
Magaña J., Amante M. H., Garcia-Aspeitia M. A., Motta V., 2018, MNRAS, 476, 1036
Marra V., Sapone D., 2018, Phys. Rev. D, 97, 083510
Montanari F., Räsänen S., 2017, J. Cosmol. Astropart. Phys., 2017, 032
Moraes P. H. R. S., 2019, Eur. Phys. J. C, 79, 674
Moresco M. et al., 2012, J. Cosmol. Astropart. Phys., 2012, 006
Moresco M. et al., 2016, J. Cosmol. Astropart. Phys., 2016, 014
Moresco M., 2015, MNRAS, 450, L16
Mörtsell E., Clarkson C., 2009, J. Cosmol. Astropart. Phys., 2009, 044
Mortsell E., Jonsson J., 2011, preprint (arXiv:1102.4485)
Oka A., Saito S., Nishimichi T., Taruya A., Yamamoto K., 2014, MNRAS, 439, 2515
Overduin J. M., Wesson P. S., 1997, Phys. Rep., 283, 303
Peebles P. J., Ratra B., 2003, Rev. Mod. Phys., 75, 559
Percival W. J., Cole S., Eisenstein D. J., Nichol R. C., Peacock J. A., Pope A. C., Szalay A. S., 2007, MNRAS, 381, 1053
Perlmutter S. et al., 1999, ApJ, 517, 565
Planck Collaboration XVI, 2014, A&A, 571, A16
Planck Collaboration XIII, 2016, A&A, 594, A13
Planck Collaboration VI, 2018, A&A, 641, A6
Randall L., Sundrum R., 1999, Phys. Rev. Lett., 83, 4690
Rapetti D., Allen S. W., Amin M. A., Bland ford R. D., 2007, MNRAS, 375, 1510
Riess A. G. et al., 1998, AJ, 116, 1009
Riess A. G. et al., 2004, ApJ, 607, 665
Riess A. G. et al., 2007, ApJ, 659, 98
Riess A. G. et al., 2016, ApJ, 826, 56
Riess A. G., Casertano S., Yuan W., Macri L. M., Scolnic D., 2019, ApJ, 876, 85
Sahni V., Starobinsky A., 2006, Int. J. Mod. Phys. D, 15, 2105
Sahni V., Wang L., 2000, Phys. Rev. D, 62, 103517

Sapone D., Majerotto E., Nesseris S., 2014, Phys. Rev. D, 90, 023012
Schlegel D., White M., Eisenstein D., 2009, Science White Papers, no. 106, astro2010: The Astronomy and Astrophysics Decadal Survey. p. 314
Schwarz G., 1978, Ann. Statist., 6, 461
Scolnic D. M. et al., 2018, ApJ, 859, 101
Shapiro C., Turner M. S., 2006, ApJ, 649, 563
Sharov G. S., Vorontsova E. G., 2014, J. Cosmol. Astropart. Phys., 2014, 057
Shiromizu T., Maeda K.-I., Sasaki M., 2000, Phys. Rev. D, 62, 024012
Simon J., Verde L., Jimenez R., 2005, Phys. Rev. D, 71, 123001
Sotiriou T. P., Faraoni V., 2010, Rev. Mod. Phys., 82, 451
Stern D., Jimenez R., Verde L., Kamionkowski M., Stanford S. A., 2010, J. Cosmol. Astropart. Phys., 2010, 008
Suzuki N. et al., 2012, ApJ, 746, 85
Szydłowski M., Krawiec A., Kurek A., Kamionka M., 2015, Eur. Phys. J. C, 75, 5
Tripp R., Branch D., 1999, ApJ, 525, 209
Valentim R., Horvath J. E., Rangel E. M., 2011a, Int. J. Mod. Phys. E, 20, 203
Valentim R., Rangel E., Horvath J. E., 2011b, MNRAS, 414, 1427
Visser M., 2004, Class. Quantum Gravity, 21, 2603
Visser M., 2005, Gen. Relativ. Gravit., 37, 1541
Volkov M. S., 2012, Phys. Rev. D, 86, 061502
von Marttens R., Marra V., Casarini L., Gonzalez J., Alcaniz J., 2019, Phys. Rev. D, 99, 043521
Wang G.-J., Wei J.-J., Li Z.-X., Xia J.-Q., Zhu Z.-H., 2017, ApJ, 847, 45
Wei J.-J., Wu X.-F., 2017, ApJ, 838, 160
Weinberg D. H., Mortonson M. J., Eisenstein D. J., Hirata C., Riess A. G., Rozo E., 2013, Phys. Rep., 530, 87
Witzemann A., Bull P., Clarkson C., Santos M. G., Spinelli M., Weltman A., 2018, MNRAS, 477, L122
Yu H., Wang F. Y., 2016, ApJ, 828, 85
Yu H., Ratra B., Wang F.-Y., 2018, ApJ, 856, 3
Zhang C., Zhang H., Yuan S., Liu S., Zhang T.-J., Sun Y.-C., 2014, Res. Astron. Astrophys., 14, 1221

This paper has been typeset from a TEX/LATEX file prepared by the author.